Iranian Journal of Analytical Chemistry
Volume 8, Issue 2, September 2021 (99-106) Origonal Research Article

مجله ایرانی شیمی تجزیه
دوره۸، شماره ۲، مهرماه ۱۴۰۰ (۱۰۶-۹۹)

Ultrasound-Assisted Synthesis of P-Doped Graphitic Carbon Nitride Nanosheets for Efficient Photodegradation of Tartrazine

Vida Haji Aghaei*, Narges Ajami
Department of Chemistry, Payame Noor University, 19395-4697, Tehran, Iran

Received: 17 August 2021 **Accepted:** 22 September 2021
DOI: 10.30473/ijac.2022.62570.1223

Abstract
In this paper, graphitic carbon nitride (g-C_3N_4) was prepared by direct pyrolysis of melamine and then used to synthesize P-doped graphitic carbon nitride nanosheets with ultrasound in phosphoric acid. This simple method helps increase the trapping of light, change the electronic property of g-C_3N_4 and prevent charge recombination in the as-prepared photocatalyst. The useful features of this method to prepare P-doped g-C_3N_4 nanosheets are its simplicity, short synthesis time, economical and environmentally friendly. The present study demonstrates the ability of phosphoric acid to synthesize P-doped g-C_3N_4 nanosheets with ultrasound, which leads to an increase in photodegradation of Tartrazine under visible light.

Keywords
Graphitic Carbon Nitride; Tartrazine; Photocatalyst; P-Doped g-C_3N_4.

1. INTRODUCTION

Organic pollutants present in industrial wastewater are of significant concern to the health of the general public. There are several established ways to remove such contaminants [1]. In recent years, there has been a growing interest in the use of semiconductors as photocatalysts for dye degradation [2, 3].

Azo dyes are a class of synthetic organic dyestuffs that are manufactured worldwide and have a variety of applications such as textiles, paper, foodstuff, and cosmetics [4]. Tartrazine is widely used in the food and drugs industries. It also has a high solubility in water. Some people are susceptible to Tartrazine as it can cause breathing difficulties. Thus, Tartrazine waste from the food and drugs industries must be treated with appropriate yet affordable technology before being released to the environment [1, 5].

In recent years, the photocatalytic degradation method has attracted increasing attention as cleaner and greener technology for removing toxic organic pollutants in water and wastewater [6]. Semiconductor photocatalyst appears to be a promising technology as it has several applications in the environmental system such as air purification, water disinfection, water purification, and hazardous waste remediation.

Graphitic carbon nitride was discovered in the 1830s [7]. In recent years, due to the unique physicochemical property and electronic band structure, graphitic carbon nitride has been developed as a metal-free and non-toxic photocatalyst with visible light response [8, 9, 10]. Graphitic carbon nitride, as an analog of graphene, has been of considerable interest due to the strong electron donor nature of nitrogen present in g-C_3N_4, which is absent in graphene [11]. It is a defect-rich, N-bridged poly (tri-s-triazine), whereby the defects and nitrogen atoms serve as active sites for electron conductivity [12]. The highly condensed tri-s-triazine ring structure makes the polymer possess high stability concerning thermal and chemical attacks and an appealing electronic structure, being a medium-gap semiconductor excitable with visible light [9, 13, 14]. The application of polymeric carbon nitride-based photocatalysts in environmental cleanup has also been demonstrated for the degradation of dyes and colorless light-weight molecules [15, 16]. In addition to this, it is a potential candidate for other applications like CO_2 reduction and hydrogen evolution [17, 18], sensors [19,20], anticorrosion coating [21,22], and can also be used in fuel cell and energy storage devices [23, 24].

In recent years, g-C_3N_4 has been used for the photocatalytic degradation of organic colors such as Rhodamine B [25, 26], Methyl Orange [27, 28], and Methylene blue [29, 30]. In most articles, phosphorus-doped in g-C_3N_4 is produced by thermal copolymerization [31, 32, 33]. In this work, the synthesis of the P-doped g-C_3N_4 nanosheets by ultrasonic g-C_3N_4 with phosphoric acid was prepared for the first time. This simple method in the short synthesis time, exhibited novel strategies to enhance the visible light photocatalytic performance of g-C_3N_4.

*Corresponding Author: vidahadji2003@gmail.com, hadji@pnu.ac.ir

2. EXPERIMENTAL

2.1. Preparation of the Photocatalyst

The g-C_3N_4 powder was synthesized with direct pyrolysis of the melamine based on the report [21]. To prepare g-C_3N_4 5 g melamine was put in a crucible and was heated in a furnace for 4 h at 550°C. Then after reached to room temperature, the pale yellow g-C_3N_4 was collected and milled to powder.

The mixture of phosphoric acid and g-C_3N_4 (1.8 g L^{-1}) was exposed to ultrasound irradiations to prepare the P-doped g-C_3N_4 nanosheets photocatalyst for 6 h. The color change from yellow to milky white was observed. Then the mixture was centrifuged for 15 min at 5000 rpm and residual dried in an oven at 60°C for 12 h to study the P-doped g-C_3N_4 nanosheets phase, morphology, composition, and structure by using field emission scanning electron microscopy and X-ray diffractometer. Then the electrochemical properties of the P-doped g-C_3N_4 nanosheets were studied by impedance spectroscopy and cyclic voltammetry.

2.2. Photocatalytic activity measurement

The photocatalytic activities were evaluated by degradation of Tartrazine solution under visible light irradiation. The bulk g-C_3N_4 (1.8 g L^{-1}) was dispersed in phosphoric acid solution (0.1mol L^{-1}) and exposed to ultrasound irradiations for 6 h. Then 20 mg L^{-1} of Tartrazine was added to photocatalyst. The mixture was stirred in the dark for 30 min to reach the adsorption-desorption equilibrium. Then the mixture was exposed to visible light for 100 min, and approximately 5 mL of it was collected at selected times during the photoreaction process and centrifuged at 5000 rpm for 10 min to separate the photocatalyst. The adsorption changes in the solutions during the photocatalytic process were investigated by spectrophotometer.

3. RESULT AND DISCUSSION

3.1. Characterization

Fig. 1 displays the XRD patterns of the pure-g-C_3N_4 and P-doped g-C_3N_4. Typically, g-C_3N_4 powder shows two diffraction peaks. One of them at about 27.3°, corresponding to the inter-planar stacking peak of the conjugated aromatic system, which could be indexed as the (002) diffraction plane. The other at about 13.1° corresponds to the in-plane structural packing motif of the tri-s-triazine units, which could be correctly indexed to the (100) diffraction plane for graphitic materials (Fig. 1a) [34].

It is worth noting that both the (002) and (100) peaks can be observed in the X-ray pattern of P-doped g-C_3N_4 nanosheets, indicating that the basic structure of g-C_3N_4 is preserved. The (002) and (100) Peaks intensities decreased for P-doped g-C_3N_4 nanosheets compared to bulk-g-C_3N_4, showing the thin and few-layered analysis (Fig. 1b) [35]. The results show that in addition to doped phosphorus to graphitic carbon nitride, secondary graphitic carbon nanosheets have also been created using this method, which improves photocatalytic efficiency.

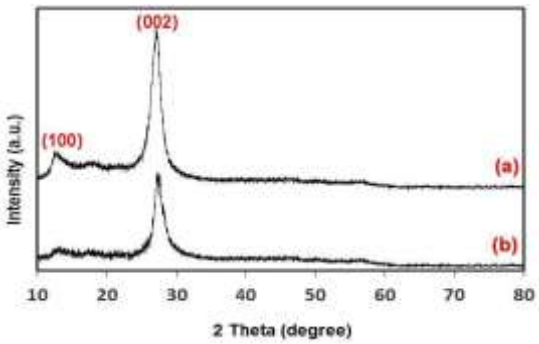

Fig. 1. XRD pattern of (a) bulk g-C_3N_4 and (b) P-doped g-C_3N_4.

In order to confirm the effect of H_3PO_4 on the morphology of the as-prepared catalyst, the morphologies of the representative samples were examined by FESEM analysis. As depicted in Fig. 2a, the g-C_3N_4 sample exhibited a layered, stacked texture surface and plate-like structure. As shown in Fig. 2b, the treatment with H_3PO4 had markedly changed the morphology of g-C_3N_4, causing the g-C_3N_4 layer structure to disappear, and the g-C_3N_4 nanosheets form [35].

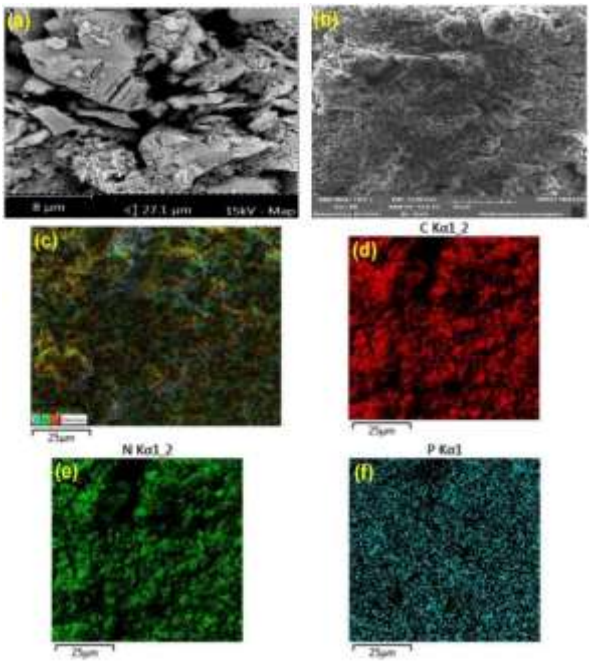

Fig. 2. FESEM images of (a) bulk g-C_3N_4, (b) P-doped g-C_3N_4 nanosheets and EDS elemental mapping images of (c) P-doped g-C_3N_4, (d) C element, (e) N element and (f) P element.

Meanwhile, the energy dispersive spectroscopy (EDS) elemental mapping of P-doped g-C_3N_4 was performed to display the distribution patterns of the components (Fig. 2c). As shown from Fig. 2(d-f), all three major elements (C, N, and P) are uniformly distributed in the P-doped g-C_3N_4 sample.

The P-doped g-C_3N_4 exhibited enhanced visible light photocatalytic performance. This synthesis method is beneficial for tuning the bandgap structure, enhancing light trapping, accelerating charges separation and inhibiting the recombination of the photo-induced electron-hole pairs.

3.2. Electrochemical Characterization

The electrochemical properties of g-C_3N_4 before and after H_3PO_4 treatment were investigated by electrochemical impedance spectroscopy. The electrochemical impedance spectroscopy measurements are carried out over a frequency domain from 100 kHz to 0.1 Hz at open circuit potential. The electrochemical impedance spectrum shown in Fig. 3A implies the decreased electron transfer resistance in P-doped g-C_3N_4 nanosheets than bulk-g-C_3N_4 because of the much smaller diameter of the semicircular Nyquist plots. Thus, the P-doped g-C_3N_4 nanosheets show improved charges separation and electronic conductivity, which result in enhanced photocatalytic activity.

Then the electrochemical responses of g-C_3N_4 were studied by measuring the cyclic voltammetric (Fig. 3B). The voltammetric response of g-C_3N_4 after H_3PO_4 treatment was significantly improved compared to HCl. The enhanced voltammetric response of p-doped g-C_3N_4 nanosheets indicates that the electronic conductivity of g-C_3N_4 improved after H_3PO_4 treatment. Therefore, in this work, g-C_3N_4 was used after H_3PO_4 treatment for the photodegradation of Tartrazine.

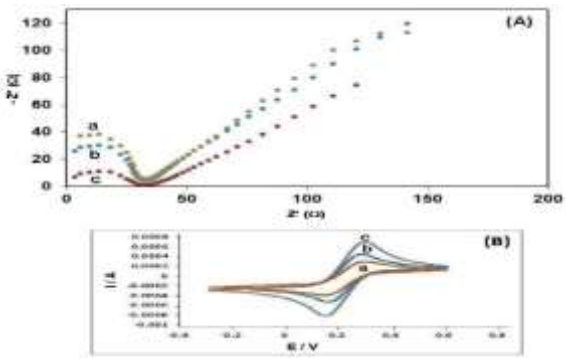

Fig. 3. (A) Electrochemical impedance spectroscopy plots and (B) Cyclic voltammograms of (a) bare (graphite pencil), (b) graphite/g-C_3N_4 treatment with HCl and (c) graphite/g-C_3N_4 treatment with H_3PO_4 in 5 mmol L^{-1} $[Fe(CN)_6]^{3-}$.

3.3. Effect of Catalyst Amount

Degradation of dye is affected by the amount of photocatalyst. Results obtained from experiments on dye degradation using different amounts of P-doped g-C_3N_4 from 1.4 to 2.2 g L^{-1} were illustrated in Fig. 4A. In the photocatalytic process, the reaction has taken place on the surface of the catalyst, so the amount of catalyst loaded into the system can affect the performance of this reaction. The increase in catalyst amount increases the number of active sites on the photocatalyst surface, thus causing an increase in the formation of the number of OH radicals that can take part in the actual discoloration of dye solution. However, the amount of degraded Tartrazine increased with catalyst loading up to 1.8 g L^{-1} but decreased after further loading. This is because excess catalysts concentration increases the turbidity of the solution, which in turn reduces the light transmission through the solution.

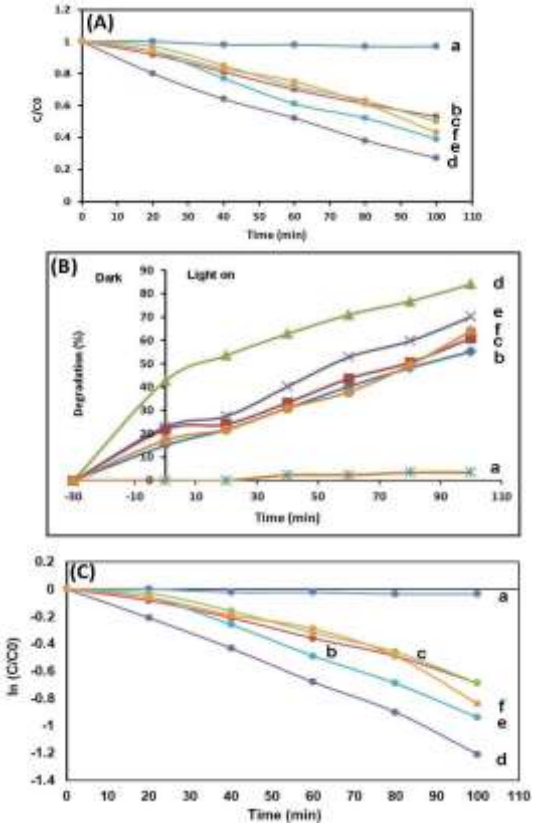

Fig. 4. (A) Photocatalytic degradation, (B) Photocatalytic degradation percentage and (C) Photodegradation rate of 20 mg L^{-1} of Tartrazine under visible light irradiation with different amounts of (a) 0, (b) 1.4, (c) 1.6, (d) 1.8, (e) 2.0 and (f) 2.2 g L^{-1} photocatalyst.

Fig. 4B shows that after 100 min, the degradation percentage was at a maximum with about 85% at 1.8 g L^{-1} of catalyst loading. Thus, the optimum amount of catalyst loading was found to be 1.8 g L^{-1}.

Also, the effect of photocatalyst amount on the Tartrazine degradation rate showed that the highest degradation rate occurred at the optimum photocatalyst amount, where the slope of the degradation plot showed the highest value (Fig. 4C). As shown in Table 1, the degradation rate of Tartrazine has presented the highest value at the optimum amount of photocatalyst. The photodegradation rate was obtained 0.0004, 0.0069, 0.007, 0.012, 0.0097 and 0.0008 min^{-1} for P-doped g-C_3N_4 nanosheets, with different concentration of 0, 1.4, 1.6, 1.8, 2.0 and 2.2 g L^{-1} of g-C_3N_4 respectively. The photocatalyst with 1.8 g-C_3N_4 showed the highest photodegradation rate. Also, the best correlation coefficient (R^2) is 0.9964 and suggests a reasonably good fit between the degradation rate of Tartrazine and time.

The photocatalytic efficiency of the P-doped g-C_3N_4 nanosheets has been compared with different photocatalysts which were shown in Table 2. This Table shows that the photodegradation time of Tartrazine is more in the reported photocatalysts. Also, the degradations have been performed either with lower dye concentration or a higher amount of photocatalyst compared to the present study. These are some of the advantages of this photocatalyst. So, the P-doped g-C_3N_4 nanosheets showed better photodegradation of Tartrazine under visible light compared to the reported photocatalysts.

3.4. Effect of electrolyte

Tartrazine photodegradation was performed in two electrolytes with different compositions, and the effect on photocatalytic performance was investigated. The photodegradation of 20 mg L^{-1} Tartrazine on g-C_3N_4 were examined in various supporting electrolytes, with the same concentration (0.1 mol L^{-1}) of phosphoric acid and hydrochloric acid. The photocatalytic properties of g-C_3N_4 were studied after H_3PO_4 and HCl ultrasonic treatment by measuring their photocatalytic performance (Fig. 5). The P-doped g-C_3N_4 nanosheets show excellent photocatalytic performance and indicate the separation efficiency of the photo-induced electron-hole pairs is further improved. The H_3PO_4 treatment not only helps to form the g-C_3N_4 nanosheets but also tunes the bandgap of g-C_3N_4. Thus, these synergistic effects lead to improved photocatalytic degradation performance of Tartrazine under visible light.

The results show that using phosphoric acid as an electrolyte increases the photocatalytic degradation performance of Tartrazine compared to hydrochloric acid. The photocatalyst was prepared in the referred supporting electrolyte for the photodegradation process.

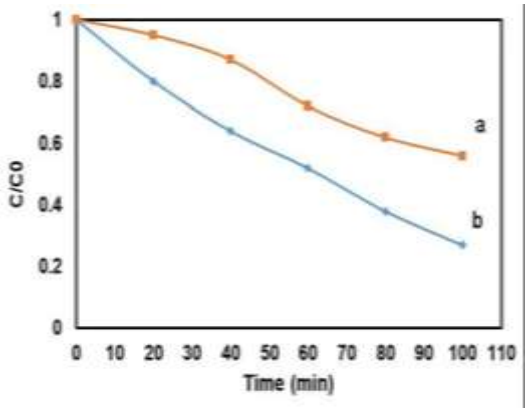

Fig. 5. Effect of electrolyte type: (a) HCl and (b) H_3PO_4 on photodegradation of Tartrazine.

Table 1. Photocatalytic degradation rate of Tartrazine with different amounts of photocatalyst under visible light.

Photocatalyst concentration (g L^{-1})	Line equation	Line slop (Tartrazine degradation rate)	R^2
0	Y = -0.0004x + 0.0007	- 0.0004	0.8851
1.4	Y = -0.0069x + 0.0389	- 0.0069	0.9858
1.6	Y = -0.007x + 0.0733	- 0.007	0.9599
1.8	Y = -0.012x + 0.0254	- 0.012	0.9964
2.0	Y = -0.0097x + 0.0805	- 0.0097	0.979
2.2	Y = -0.008x + 0.0876	- 0.008	0.9172

Table 2. Comparision of different photocatalysts in photodegradation of Tartrazine.

Photocatalyst	Concentration of Tartrazine	Amount of catalyst	Irradiation time (min)	Light source	% Degradation	Reference
Cu-modified silicon nanowires	1.035×10^{-5} mol L^{-1}	NA	200	UV	67.45	[36]
$LaFeO_3$/ ZnO	10 mg L^{-1}	3 g L^{-1}	180	UV	84.00	[37]
TiO_2 on magnetic particles	1×10^{-5} mol L^{-1}	2 g L^{-1}	120	UV	80.00	[38]
Periwinkle shell ash	30 mg L^{-1}	5 g L^{-1}	60	UV	85.00	[39]
p-doped g-C_3N_4 nanosheets	20 mg L^{-1}	1.8 g L^{-1}	100	Visible	85.00	Present work

3.5. Effect of adsorption time on the photocatalytic behavior of the g-C_3N_4

The relationship between photocatalytic performance and adsorption time of Tartrazine, on the P-doped g-C_3N_4 nanosheets surface, with 1.8 g L^{-1} concentration in the dark at 25°C was investigated in a range of 15-45 min (Fig. 6). As a result, the adsorption of dye on the surface is altered, thereby causing a change in the reaction rate. Compared with the bulk-g-C_3N_4, the absorption of the band edge of P-doped g-C_3N_4 nanosheets show significant enhancement in photocatalytic removal of Tartrazine. The synergistic effect between increasing the specific surface area and the number of active sites in the photocatalyst increases the amount of dye adsorbed on the photocatalyst surface, and as a result, increases the photocatalytic degradation performance. After reaching the equilibrium time of 30 min, the photocatalyst adsorption rate decreases with increasing time up to 45 min, indicating that the optimum contact time for Tartrazine adsorption is 30 min.

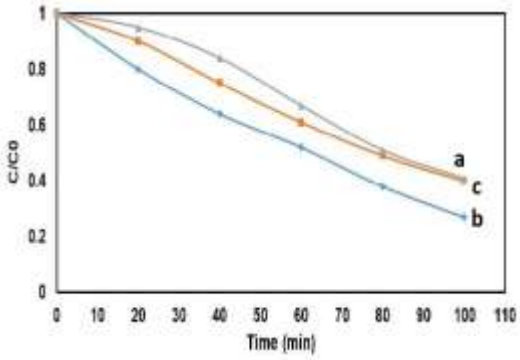

Fig. 6. Effect of adsorption time: (a) 15, (b) 30, (c) 45 min on photodegradation of Tartrazine.

3.6. Effect of Ultrasonic time on the photocatalytic behavior of the g-C_3N_4

The relationship between photocatalytic performance and ultrasonic time of g-C_3N_4 in phosphoric acid was investigated in a range of 4.0-8.0 hours. The photocatalytic performance of ultrasonic g-C_3N_4 in phosphoric acid compared to the bulk-g-C_3N_4 was enhanced. This strategy is beneficial to increase the surface area, enhance light trapping, accelerate charges separation and create more active sites.

The ultrasonic g-C_3N_4 in phosphoric acid shows significant enhancement in photocatalytic removal of Tartrazine. As shown in Fig. 7, the photocatalytic performance exhibits a significant enhancement by increasing the ultrasonic time from 4.0 to 6.0 hours, but this effect is constant with increasing time to 8.0 h. The photocatalytic degradation rate remains almost unchanged after 6.0 h. So it was selected as the best ultrasonic time for g-C_3N_4. After this time, P-doped g-C_3N_4 nanosheets are formed, which are shown by FESEM images (Fig. 2).

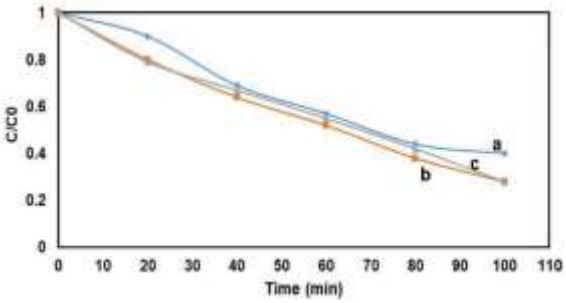

Fig. 7. Effect of ultrasonic time: (a) 4.0, (b) 6.0, (c) 8.0 hour on photodegradation of Tartrazine.

4. CONCLUSION

In summary, graphitic carbon nitride (bulk-g-C_3N_4) was fabricated by direct pyrolysis of melamine and then was sonicated in phosphoric acid to prepare P-doped g-C_3N_4 nanosheets. In this simple method, the P-doped g-C_3N_4 nanosheets would enhance light trapping and increase charge separation, which makes it a more efficient photocatalyst than a bulk g-C_3N_4 counterpart to remove Tartrazine. The performance of the photocatalytic activity is correlated to the structure of g-C_3N_4, and the results showed that the p-doped g-C_3N_4 nanosheets enhanced the photodegradation of Tartrazine under visible light.

Several characterizations investigated the changes in the crystal structure, microstructure, and optical properties of g-C_3N_4. The useful features of this method to prepare the P-doped g-C_3N_4 nanosheets are its simplicity, short synthesis time, economical and environmentally friendly. The present study demonstrates the ability of phosphoric acid to prepare the P-doped g-C_3N_4 nanosheets with ultrasound. We have obtained good results for P-doping based on this method, which can be used for different samples in the future, especially carbon allotropes.

ACKNOWLEDGEMENTS

In this paper, we thank of Payame Noor University for providing laboratory facilities for this research.

REFERENCES

[1] S.K. AL-Dawery, Photo-Catalysted Degradation of Ttartrazine compound in waste water using TiO_2 and UV lights, *ESTEC* 8 (2013) 683-691.

[2] H.A.A. Hashimi, A. Rahmanmohamed and L. K. Teong, Solar photocatalytic degradation of

tartrazine using titanium dioxide, *J. Teknol.* 35 (2001) 31–40.

[3] W.J. Ong, L.L. Tan, Y. H. Ng, S.T. Yong and S.P. Chai, Graphitic carbon nitride (g-C_3N_4) based photocatalysts for artificial photosynthesis and environmental remediation: are we a step closer to achieving sustainability. *Chem. Rev.* 116(2016) 7159-7329.

[4] R. Jain and S. Sikarwar, Photocatalytic and adsorption studies on the removal of dye Congo red from wastewater, *Int. J. Environ. Pollut.* 27 (2006) 158-178.

[5] H.A. Abdullah Hashim, A. Rahman Mohamed and L.K. Teong, Solar photocatalytic degradation of tartrazine using titanium dioxide, *J. Teknol. Dis*. 35(2001) 31–40.

[6] R. Ameta, S. Benjamin, A. Ameta and S.C. Ameta, Photocatalytic degradation of organic pollutants: a review, *Mater. Sci. Forum*. 734 (2013) 247-272.

[7] Y.T. Yew, C.S. Lim, A.Y.S. Eng, J. Oh, S. Park and M. Pumera, Electrochemistry of layered graphitic carbon nitride synthesised from various precursors: searching for catalytic effects, *ChemPhys. Chem*. 17 (2016) 481-488.

[8] H.Y. Xu, L.C. Wu, H. Zhao, L.G. Jin and S.Y. Qi, Synergic effect between adsorption and photocatalysis of metal Free g-C3N4 derived from different precursors, *Plos. one* 10 (2015) e0142616.

[9] Y. Cui, J. Huang, X. Fu and X. Wang, Metal-free photocatalytic degradation of 4-chlorophenol in water by mesoporous carbon nitride semiconductors, *Catal. Sci. Technol*. 2 (2012) 1396–1402.

[10] W.K. Jo and H.J. Yoo, Combination of ultrasound-treated 2D g-C3N4 with Ag/black TiO2 nanostructure for improved photocatalysis, *Ultrason*. *Sonochem*. 42 (2018) 517-525.

[11] H. Gu, T. Zhou and G. Shi, Synthesis of graphene supported graphene-like C_3N_4 metal-free layered nanosheets for enhanced electrochemical performance and their biosensing for biomolecules, *Talanta* 132 (2015) 871–876.

[12] H.L. Lee, Z. Sofer, V. Mazánek, J. Luxa, C.K. Chua and M. Pumera, Graphitic carbon nitride: Effects of various precursors on the structural morphological and electrochemical sensing properties, *Appl. Mater. Today* 8(2016) 150–162.

[13] Y. Wang, X. Wang and M. Antonietti. Polymeric graphitic carbon nitride as a heterogeneous organocatalyst: From photochemistry to multipurpose catalysis to sustainable chemistry, *Angew. Chem. Int. Ed*. 51 (2012) 68–89.

[14] P. Balasubramanian, M. Annalakshmi, S.M. Chen and T.W. Chena, Sonochemical synthesis of molybdenum oxide (MoO_3) microspheres anchored graphitic carbon nitride (g-C_3N_4) ultrathin sheets for enhanced electrochemical sensing of Furazolidone, *Ultrason. Sonochem*. 50 (2019) 96-104.

[15] G. Dong, Z. Ai and L. Zhang, Efficient anoxic pollutant removal with oxygen functionalized graphitic carbon nitride under visible light, *RSC Adv*. 4 (2014) 5553–5560.

[16] L. Ge, Synthesis and photocatalytic performance of novel metal-free g-C3N4 photocatalysts, *Mater. lett*. 65 (2011) 2652–2654.

[17] S. Yin, J. Han, T. Zhou and R. Xu, Recent progress in g-C_3N_4 based low cost photocatalytic system: activity enhancement and emerging applications, *Catalysis Science & Technology* 5 (2015) 5048-5061.

[18] L.Y. Chen and W.D. Zhang, In_2O_3/g-C_3N_4 composite photocatalysts with enhanced visible light driven activity, *Appl. Sur. Sci*. 301 (2014) 428–435.

[19] H. Zhang, Q. Huang, Y. Huang, F. Li, W. Zhang, C. Wei, J. Chen, P. Dai, L. Huang, Z. Huang, L. Kanga, S. Hua and A. Hao, Graphitic carbon nitride nanosheets doped graphene oxide for electrochemical simultaneous determination of ascorbic acid, dopamine and uric acid, *Electrochimi. Acta* 142 (2014) 125–131.

[20] M. Afshari, M. Dinari and M.M. Momeni, Ultrasonic irradiation preparation of graphitic-C_3N_4/polyaniline nanocomposites as counter electrodes for dye-sensitized solar cells, *Ultrason. Sonochem*. 42 (2018) 631-639.

[21] M.A. Karimi, V.H. Aghaei, A. Nezhadali and N. Ajami, Investigation of copper corrosion in sodium chloride solution by using a new coating of polystyrene/g-C_3N_4, *J. Mater. Sci.: Mater. Electron*. 30 (2019) 6300-6310.

[22] S. Zuo, Y. Chen, W. Liu, C. Yao, Y. Li, J. Ma, Y. Kong, H. Mao, Z. Li and Y. Fu, Polyaniline/g-C_3N_4 composites as novel media for anticorrosion coatings, *J. Coat. Technol. Res*. 14 (2017) 1307–1314.

[23] Y. Fu, J. Zhu, C. Hu, X. Wu and X. Wang, covalently coupled hybrid of graphitic carbon nitride with reduced graphene oxide as a superior performance lithium-ion battery anode, *Nanoscale* 6 (2104) 12555-12564.

[24] Y. Zheng, J. Liu, J. Liang, M. Jaroniec and S.Z. Qiao, Graphitic carbon nitride materials:

controllable synthesis and applications in fuel cells and photocatalysis, *Energy Environ. Sci*. 5 (2012) 6717–6731.

[25] S.C. Yan, Z.S. Li and Z.G. Zou, Photodegradation of Rhodamine B and Methyl Orange over Boron-doped g-C_3N_4 under visible light irradiation, *Langmuir* 26 (2010) 3894–3901.

[26] B. Chai, J. Yan, C. Wang, Z. Ren and Y. Zhu, enhanced visible light photocatalytic degradation of Rhodamine B over phosphorus doped graphitic carbon nitride, *Appl. Surf. Sci.* 391 (2016) 376-383.

[27] L. Ge, C. Han and J. Liu, Novel visible light-induced g-C_3N_4/Bi_2WO_6 composite photocatalysts for efficient degradation of Methyl Orange, *Appl. Catal. B-environ*. 108–109 (2011) 100– 107.

[28] Y. Guo, R. Wang, P. Wang, Y. Li and C. Wang, developing polyetherimide/graphitic carbon nitride floating photocatalyst with good photodegradation performance of methyl orange under light irradiation, *Chemosphere* 179 (2017) 84-91.

[29] L. Song, S. Zhang, X. Wu and Q. Wei, A metal-free and graphitic carbon nitride sonocatalyst with high sonocatalytic activity for degradation methylene blue, *Chem. Eng. J*. 184 (2012) 256– 260.

[30] Z. Mo, X. She, Y. Li, L. Liu, L. Huang, Z. Chen, Q. Zhang, H. Xu and H. Li, Synthesis of g-C_3N_4 prepared at different temperatures for superior visible/UV photocatalytic performance and photoelectrochemical sensing of MB solution, *RSC Advances* 5 (2015) 101552-101562.

[31] L. Jiang, X. Yuan, G. Zeng, X. Chen, Z. Wu, J. Liang, J. Zhang, H. Wang and H. Wang, Phosphorus and Sulfur-codoped g-C_3N_4: Facile preparation, mechanism insight, and application as efficient photocatalyst for tetracycline and Methyl Orange degradation under visible light irradiation, *Chem. Eng*. 5 (2017) 5831−5841.

[32] W. Zhang, J. Zhang, F. Dong and Y. Zhang, Facile synthesis of in-situ phosphorus-doped g-C_3N_4 with enhanced visible light photocatalytic property for NO purification, *RSC Advances* 6 (2016) 88085-88089.

[33] R. Ran, T.Y. Ma, G. Gao, X.W. Du and S.Z. Qiao, Porous P-doped graphitic carbon nitride nanosheets for synergistically enhanced visible light photocatalytic H_2 production, *Energ. & Envir. ment.Sci.* 8 (2015) 3708-3717.

[34] R. You, H. Dou, L. Chen, S. Zheng and Y. Zhang, Graphitic carbon nitride with S and O co-doping for enhanced visible light photocatalytic performance, *RSC Adv*. 7 (2017) 15842–15850.

[35] J. Tong, L. Zhang, F. Li, K. Wang, L. Han and S. Cao, Rapid and high-yield production of g-C_3N_4 nanosheets via chemical exfoliation for photocatalytic H_2 evolution, *RSC Advances* 5 (2015) 88149-88153.

[36] S. Naama, T. Hadjersi, H. Menari, G. Nezzal, L. B. Ahmed and S. Lamrani, Enhancement of the tartrazine photodegradation by modification of silicon nanowires with metal nanoparticles, *Mater. Res. Bull*. 76 (2016) 317-326.

[37] V. Vaiano, G. Iervolino and D. Sannino, Photocatalytic removal of Tartrazine dye from aqueous samples on $LaFeO_3$/ZnO photocatalysts, *Chem. Eng. Trans*. 52 (2016) 847-852.

[38] C.L. Heredia, E.L. Sham and E.M. Farfán-Torres, Tartrazine degradation by supported TiO_2 on magnetic particles, *Revista Matéria*. 20 (2015) 668– 675.

[39] N.A. Amenaghawon, J.O. Osarumwense, F. A. Aisien and O.K. Olaniyan, Preparation and Investigation of the photocatalytic properties of periwinkle sheel ash for Tartrazine decolourisation, *JMES*. 7 (2014) 1070-1084.

سنتز نانوورقه‌های کربن نیترید گرافیتی دوپ شده با فسفر به کمک اولتراسونیک برای تخریب کارآمد تارترازین

ویدا حاجی آقایی*، نرگس عجمی

گروه شیمی، دانشکده علوم، دانشگاه پیام نور، تهران، ایران

تاریخ دریافت: ۲۶ مرداد ۱۴۰۰ تاریخ پذیرش: ۳۱ شهریور ۱۴۰۰

چکیده

در این مقاله، کربن نیترید گرافیتی از طریق پیرولیز مستقیم ملامین تهیه شد و سپس برای سنتز نانو ورقه های کربن نیترید گرافیتی دوپ شده با فسفر در اسید فسفریک با اولتراسونیک مورد استفاده قرار گرفت. این روش ساده به افزایش جذب نور، تغییر خواص الکترونیکی کربن نیترید گرافیتی و جلوگیری از باز ترکیب بار در فوتوکاتالیست تهیه شده کمک کرد. از ویژگی های مفید این روش در تهیه نانو ورقه های کربن نیترید گرافیتی دوپ شده با فسفر می توان به سادگی، زمان سنتز کوتاه، مقرون به صرفه و سازگار با محیط زیست بودن آن اشاره کرد .مطالعه حاضر توانایی اسید فسفریک برای سنتز نانو ورقه های کربن نیترید گرافیتی دوپ شده با فسفر را با استفاده از امواج اولتراسونیک نشان می دهد، که این امر منجر به افزایش تخریب نوری تارترازین تحت نور مرئی شد.

واژه‌های کلیدی

کربن نیترید گرافیتی؛ تارترازین؛ فوتوکاتالیست؛ نانو ورقه‌های کربن نیترید گرافیتی دوپ‌شده با فسفر.